designs

MDPI

Article

Impact of Diffuser Location on Thermal Comfort Inside a Hospital Isolation Room

Mustafa Alkhalaf [1,*], Adrian Ilinca [2,*], Mohamed Yasser Hayyani [1] and Fahed Martini [2]

[1] Wind Energy Research Laboratory, The University of Quebec at Rimouski, Rimouski, QC G5L 3A1, Canada; mohamedyasser_hayyani@uqar.ca
[2] Mechanical Engineering Departement, École de Technologie Supérieure, Montreal, QC H3C 1K3, Canada; fahed.martini@etsmtl.ca
* Correspondence: mustafa.alkhalaf@uqar.ca (M.A.); adrian.ilinca@etsmtl.ca (A.I.)

Abstract: Thermal comfort is increasingly recognized as vital in healthcare facilities, where patients spend 80–90% of their time indoors. Sensing, controlling, and predicting indoor air quality should be monitored for thermal comfort. This study examines the effects of ventilation design on thermal comfort in hospital rooms, proposing four distinct ventilation configurations, each with three airflow rates of 9, 12, and 15 Air Changes per Hour (ACH). The study conducted various ventilation simulation scenarios for a hospital room. The objective is to determine the effect of airflow and the diffuser location distribution on thermal comfort. The Reynolds-Averaged Navier–Stokes (RANS) equations, along with the k–ε turbulence model, were used as the underlying mathematical representation for the airflow. The boundary conditions for the simulations were derived from the ventilation standards set by the American Society of Heating, Refrigerating, and Air-Conditioning Engineers (ASHRAE) and insights from previous studies. Thermal comfort and temperature distribution were assessed using indices like Predicted Percentage Dissatisfaction (PPD), Predicted Mean Vote (PMV), and Air Diffusion Performance Index (ADPI). Although most of the twelve scenarios failed to attain thermal comfort, two of those instances were optimal in this simulation. Those instances involved the return diffuser behind the patient and airflow of 9 ACH, the minimum recommended by previous studies. It should be noted that the ADPI remained unmet in these cases, revealing complexities in achieving ideal thermal conditions in healthcare environments. This study extends the insights from our prior research, advancing our understanding of ventilation impacts on thermal comfort in healthcare facilities. It underscores the need for comprehensive approaches to environmental control, setting the stage for future research to refine these findings further.

Keywords: thermal comfort; air quality; CFD Simulation; PPD; PMV; ADPI; isolation room

Citation: Alkhalaf, M.; Ilinca, A.; Hayyani, M.Y.; Martini, F. Impact of Diffuser Location on Thermal Comfort Inside a Hospital Isolation Room. *Designs* **2024**, *8*, 19. https://doi.org/10.3390/designs8020019

Academic Editor: Min-Hwi Kim

Received: 26 December 2023
Revised: 1 February 2024
Accepted: 7 February 2024
Published: 20 February 2024

1. Introduction

Thermal comfort is crucial in maintaining a comfortable environment in enclosed spaces, particularly in hospitals, where the focus is on effective contaminant removal. Residents of these buildings, especially those with health issues, are sensitive to extreme temperatures. The stress experienced in a hospital setting can lead to adverse effects such as anxiety, depression, stress, agitation, and tiredness [1]. Creating a relaxing atmosphere for patients can contribute to their rapid recovery [2,3]. However, assessing thermal comfort is complex, as multiple factors, such as temperature, relative humidity, and airflow, influence an individual's perception [4].

Academic scientists and industrial engineers are exploring ways to improve the design of hospital wards by controlling the temperature, humidity, contaminants, and velocity of the supplied air and modifying the diffuser's locations [5] Although it is a problematic issue, little previous research has focused on hospitalized patients as subjects. The American Society of Heating, Refrigerating, and Air-Conditioning Engineers (ASHRAE) has

defined thermal comfort as "the condition of the mind in which satisfaction is expressed to the existing environment" [6]. Consequently, it is crucial to understand that achieving optimal thermal comfort requires a multifaceted approach, which considers factors beyond temperature control, such as airflow dynamics and air quality. Successfully integrating these aspects into ventilation design is essential to fostering an environment conducive to comfort and healing in the hospital setting.

Different ventilation methods, such as natural, mechanical, and hybrid approaches, can regulate airflow and provide thermal comfort within a structure. Mechanical ventilation equipment such as fans and exhaust ducts are commonly used to introduce and remove air [7]. While occupants' attention is immediately drawn to thermal comfort during ventilation system operation, poor air quality may take longer to be noticed. Thermal comfort relates explicitly to temperature and related factors, and indoor air quality can indirectly influence the perceived comfort level. For ventilation to be technically possible in a space with high temperatures, it is essential to provide an adequate airflow level. Creating a stagnant layer of ambient air helps disperse metabolic heat into the surroundings. During high temperatures, it is beneficial to keep the stagnant layer close to the ground and above the occupied cooling zone [8]. However, no single ventilation design solution can consistently solve thermal problems and remain cost-effective. Therefore, effective control strategies are crucial for feasible and cost-effective ventilation system operations [5].

Several studies have investigated the impact of various factors on thermal comfort. For instance, the thermal comfort of an office located in the city center of Krakow (southern Poland) was studied by Borowski et al. [9] to determine the impact of the type of air diffusers on the operation of the air conditioning system. Tests were carried out with different diffusers, with nozzles and adjustable nozzles, which were part of the office's air conditioning system. Researchers discovered that the air velocity in a room is just as critical as the temperature and humidity values, especially in the inhabited zone, for determining the microclimate and the comfort levels in that space [5,8,9]. In addition, incorrect selection of the type or location of air conditioning system components can contribute to local discomfort for building occupants.

Computers and numerical algorithms have advanced rapidly in recent years, making CFD techniques a reasonable alternative to mathematical models and in specific cases of experimental work. As a result, in recent years, engineers and scientists have made extensive use of CFD models in their work [10]. SolidWorks software (2023 SP5) developed a 3D digital simulation tool for predicting human comfort levels. Prabhakaran et al. [11] added the heat source model to ventilation to assess human comfort factors and indoor air temperature. Net person's heat load, coolant heat source, and solar radiation are considered. According to ASHRAE, the PMV and PPD indicators' results are respectable compared to previous studies on human comfort levels. It was found in a survey of Hong Kong nursing homes by Kainaga et al. [12] that when the PMV was negative, the residents were agnostic to changes in temperature, which means that they hardly noticed if the temperature went slightly up or down.

Hwang et al. [13] performed a 3D CFD (Computational Fluid Dynamics) modeling study in a hospital operating room. The resulting airflow velocity and temperature were used in the PMV calculations. The location of the exhaust air grilles did not affect the thermal comfort. Still, it was observed that locating the supply air grilles closer to the vertical midline of the room wall improved overall performance.

By presenting the environmental parameters of five separate technical HVAC (Heating, Ventilation, and Air Conditioning) standards and guidelines, Van Gaever et al. [14] highlighted the discrepancy between the thermal comfort standard ISO 7730 and the environmental parameters defined by the technical HVAC standards. It was also established that the operating room's current HVAC systems did not provide a suitable thermal environment for all the surgical staff. Therefore, an effectively planned inlet and outlet configuration are crucial for thermal comfort.

In order to analyze the airflow into two distinct linear diffuser designs, the office building's air velocity was measured and used to analyze the airflow into two distinct linear diffuser designs [9]. The effect of airflow fluctuations on user comfort was analyzed. The findings highlight the significance of air movement and its effect on user comfort. The risk of a draught in the occupied zone can be increased by making a poor selection in diffuser type or placement.

ASHRAE standards defined some rules for space air diffusion, trying to guide the designers. For example, they mention that the outlet diffuser should be located on the side of the room away from the supply diffuser to reduce short-circuiting of supplied air [15].

Cheng, Lin, and Fong [16] investigated thermal comfort in a stratum-ventilated environmental chamber to determine the effect of supply airflow rate and temperature on thermal comfort. The results showed that at 27 °C, there was a slight change in heat perception and draught, although the supply airflow rate was increased from 7 ACH (Air Change per Hour) to 17 ACH. According to Bolashikov et al., various healthcare facility ventilation designs provide minimum ventilation equivalent to 12 ACH for isolation rooms [17].

In this research, we used CFD to model several scenarios for a hospital room ventilation system with design and flow rate modifications. These simulations, employing the RANS equations and the k–ε turbulence model, were based on data collected from previous studies. The objective is to determine the effect of airflow and the diffuser location distribution on thermal comfort.

In our preceding research [18], we investigated various ventilation designs in a hospital room, focusing on the role of airflow rates and diffuser locations in removing airborne contaminants, mainly CO_2. This study highlights the critical role of outlet positioning in enhancing air quality. Building upon these insights, our current investigation focuses on analyzing the impact of these ventilation configurations on thermal comfort within hospital rooms. Departing from our initial emphasis on contaminant elimination efficiency, the present research examines how different ventilation configurations influence thermal conditions and air distribution, factors vital for patient comfort and health. This transition from focusing on air quality to thermal comfort provides a broader understanding of the consequences of distinct ventilation strategies in healthcare facilities.

Previous studies have not clarified the diffuser's location and role in achieving thermal comfort. In addition, there is no accurate amount of airflow to commit. In this research, we have tried to investigate many designs of diffuser patterns and the recommended airflow. Moreover, the results included the ADPI, owing to considering significant factors related to our study such as air velocity, temperature, and turbulence, to evaluate the uniformity of air distribution in a given space.

The first section of this article serves as an overview of the topic. It includes a review of the literature on ventilation measuring techniques, focusing on the effect of diffusers on the occupant's comfort. Next, the methodology section outlines the control domain, boundary conditions, and mesh setting. Validation, data, and analysis are discussed in the results section. Finally, the main findings are presented in the conclusion.

2. Methodology

2.1. Governing Equations

Previous publications have established that the Reynolds-Averaged Navier–Stokes approach is adequate for modeling airflow in closed spaces [19]. Two additional partial differential equations associated with the k–ε turbulence model complete mathematical closure. We use the general laws of mass, angular momentum, and energy conservation written in a cartesian frame (SolidWorks Flow Simulation) [20,21]. In a previously published paper in the same journal, the authors presented the detailed physical model, flow equations, and turbulence model implementation [18]. Building on our previous work [18], this research advances the computational approach. While retaining the foundational (CFD) framework, including the Reynolds-Averaged Navier–Stokes (RANS) equations and k–ε turbulence model, our current focus shifts toward a comprehensive thermal comfort

analysis. We have refined our methodology by incorporating detailed comfort criteria such as Predicted Mean Vote (PMV), Predicted Percentage Dissatisfaction (PPD), Draft Temperature, and Air Diffusion Performance Index (ADPI). This approach extends our previous work on air quality and contaminant removal. It enriches our understanding of the thermal dynamics in hospital settings, thus providing a more holistic view of environmental control in healthcare facilities.

2.2. Comfort Criteria

When designing occupied spaces and their HVAC systems, the comfort criteria determine whether the environmental conditions are acceptable in general thermal comfort and air quality. The fluid flow (air) is simulated to detect the comfort parameters by thermal sensation and degree of discomfort (thermal dissatisfaction) for people exposed to moderate thermal environments [20]. In this research, we use multiple criteria, as described below.

2.2.1. Predicted Mean Vote (PMV)

PMV is an indicator that predicts the average voice value of a large group of people on a 7-point thermosensitive scale (−3 to +3) where −3 indicates cold, +3 indicates heat, and 0 represents normal temperature, according to the human body. Thermal equilibrium is reached when the body's internal heat production equals the heat loss to the environment. Therefore, in a temperate environment, the human thermoregulation system will automatically attempt to adjust the skin temperature and sweat secretion to maintain thermal balance [22]. *PMV* is defined as follows:

$$\begin{aligned} PMV = \left(0.303e^{-0.036M} + 0.028\right).\{(M-W) - 3.0{\cdot}10^{-3}[5733 - 6.99(M-W) - P_a] - 0.42[(M-W) - 58.15] - 1.7 \\ {\cdot}10^{-5}M(5867 - P_a) - 0.0014M(34 - T_a) - 3.96{\cdot}10^{-8}f_{cl}\left[(T_{cl}+273)^4 - (T_r+273)^4\right] \\ -f_{cl}h_c(T_{cl} - T_a)\} \end{aligned} \quad (1)$$

where:

$$T_{cl} = 35.7 - 0.028(M-W) - I_{cl}\left\{3.96{\cdot}10^{-8}f_{cl}\left[(T_{cl}+273)^4 - (T_r+273)^4\right] + f_{cl}h_c(T_{cl} - T_a)\right\} \quad (2)$$

$$h_c = max\left\{2.38(T_{cl} - T_a)^{0.25}, 12.1\sqrt{V}\right\} \quad (3)$$

$$f_{cl} = \begin{cases} 1.00 + 1.29I_{cl}, \ for\ I_{cl} \le 0.078\frac{\mathrm{m}^2}{\mathrm{kW}} \\ 1.00 + 0.645I_{cl}, \ for\ I_{cl} > 0.078\frac{\mathrm{m}^2}{\mathrm{kW}} \end{cases} \quad (4)$$

where: M, the metabolic rate ($\mathrm{W/m^2}$ of body surface), at which an organism's metabolism transforms chemical energy into heat and physical tasks (it is set by default at 70 $\mathrm{W/m^2}$); W is the external work ($\mathrm{W/m^2}$ of body surface), represents the effective mechanical force (the default value is 0 $\mathrm{W/m^2}$); I_{cl} is the thermal resistance of the clothes $\left(\mathrm{m^2K/W}\right)$. The resistance to heat transmission offered by the ensemble is satisfactory. Clothing insulation is measured by its ability to prevent heat loss from the wearer's entire body, which includes the feet and hands. Typical thermal resistance values for a particular clothing group is set by default to 0.11 $\mathrm{m^2K/W}$. Further, f_{cl} is the ratio of the dressed surface to the bare surface, T_a is the air temperature (K), T_r is the mean radiant temperature (K), V is the relative air velocity (m/s), P_a is the measure of the partial water vapor pressure based on the saturation curve, h_c is the convective heat transfer coefficient ($\mathrm{W/m^2/K}$), T_{cl} is the surface temperature of the garment (K).

2.2.2. The Predicted Percentage of Dissatisfaction (PPD)

PPD provides information on thermal dissatisfaction by estimating the percentage of occupants likely to feel too hot or cold in a given environment [22]. The following equation gives it:

$$PPD = 100 - 95EXP\left(-0.03353PMV^4 - 0.2179PMV^2\right) \quad (5)$$

2.2.3. Draft Temperature

It indicates the degree to which a given location in the occupied zone deviates from the baseline temperature. It is defined as a sensation of either cold or heat at a specific location on the body due to the air's temperature and velocity, with humidity and radiation considered constant.

The draft temperature T_d is defined as follows:

$$T_d = T - T_m - 7.6553\ (V - 0.1524) \quad (6)$$

where:

T is the local fluid temperature $(^{\circ}\mathrm{C})$.

T_m is the average fluid temperature within the control space $(^{\circ}\mathrm{C})$.

V is the local fluid velocity $(\mathrm{m/s})$.

2.2.4. Air Diffusion Performance Index (ADPI)

ADPI represents the area percentage where the Draft Temperature is between -1.7 and 1.1 °C, and Air Velocity is less than 0.35 (m/s).

2.3. Geometrical Model and Meshing

A hospital room model was created as part of the current study. Three elements are considered inside the room: the bed, the healthcare worker (HCW), and the patient. Room dimensions are 5 m in length, 4 m in width, and 2.8 m in height. Manikin's height is 1.7 m and its width is 0.6 m. The bed is 2.3 m long, 0.9 m in width, and 0.4 m in height. As illustrated in Figure 1, three lights are installed on the ceiling. The two air diffusers, the inlet, and the outlet, are rectangular with 0.4×0.4 m^2 dimensions. The diffusers' positions are modified according to four different designs to explore the effect on thermal comfort. We also study the influence of three different airflows. Figure 2a shows cases 1 (9 ACH), 2 (12 ACH), and 3 (15 ACH) chosen by [23], where the inlet and outlet are located on the roof. The inlet is 1 m away from the side wall, and the outlet is on the other side, 0.5 m from the side wall. For cases 4 (9 ACH), 5 (12 ACH), and 6 (15 ACH), the inlet is behind the HCW, and the outlet is in front of the HCW, at a distance of 0.5 m from the floor and roof, respectively, detailed in Figure 2b. This design has been proposed in reference [24]. Figure 2c illustrates the geometry for cases 7 (9 ACH), 8 (12 ACH), and 9 (15 ACH) with the air inlet at 0.5 m from the roof at the left of the HCW and air outlet at 1 m from the floor at the right of the HCW. In cases 10 (9 ACH), 11 (12 ACH), and 12 (15 ACH), the air outlet is moved and located close to the floor with a distance of 0.5 m, as shown in Figure 2d. The last two designs are recommended in reference [25]. For each geometry illustrated in Figure 2, we consider three airflows of 9, 12, and 15 ACH.

This investigation uses a tetrahedral-structured grid constructed with the flow simulation software SolidWorks [20]. This grid successfully captured the thermal environment's behavior. Cells are rectangular parallelepipeds with a set of orthogonal planes created by dividing the domain into a computational mesh along the axes of the cartesian global coordinate system. Initially, the original boundary-containing parallelepiped cells are subdivided into several smaller sections. First, the domain is partitioned into slices perpendicular to the axes of the Global Coordinate System using parallel planes to create the coarse-level mesh used throughout the rest of the procedure. Next, the local mesh is refined by splitting a rectangular computational mesh cell into eight cells through three orthogonal planes that divide the cell's edges into halves, as illustrated in Figure 3. In this study, two mesh sizes

are used. First, a fine mesh (local refinement) is used around the occupants, the diffusers, and the lamps at high temperatures. The coarse mesh is used everywhere else.

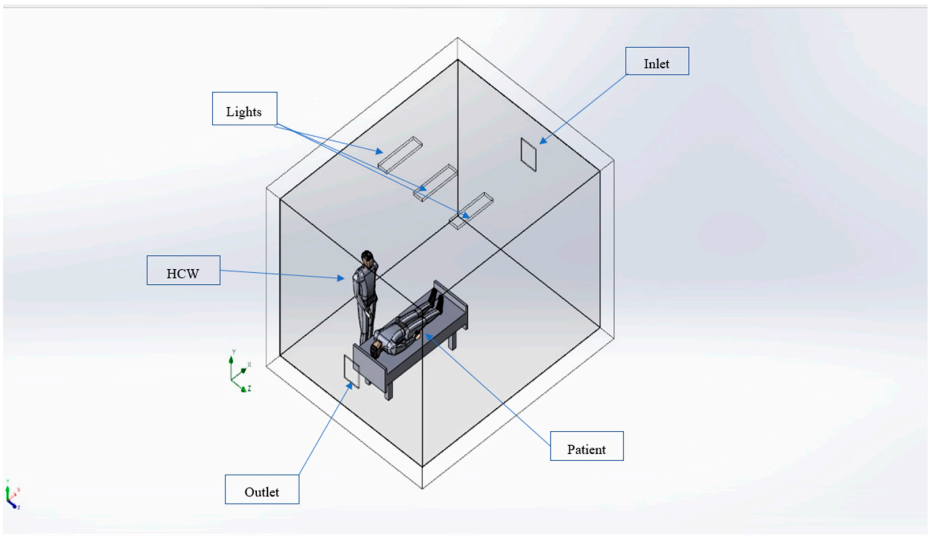

Figure 1. Isolation Room and its Content.

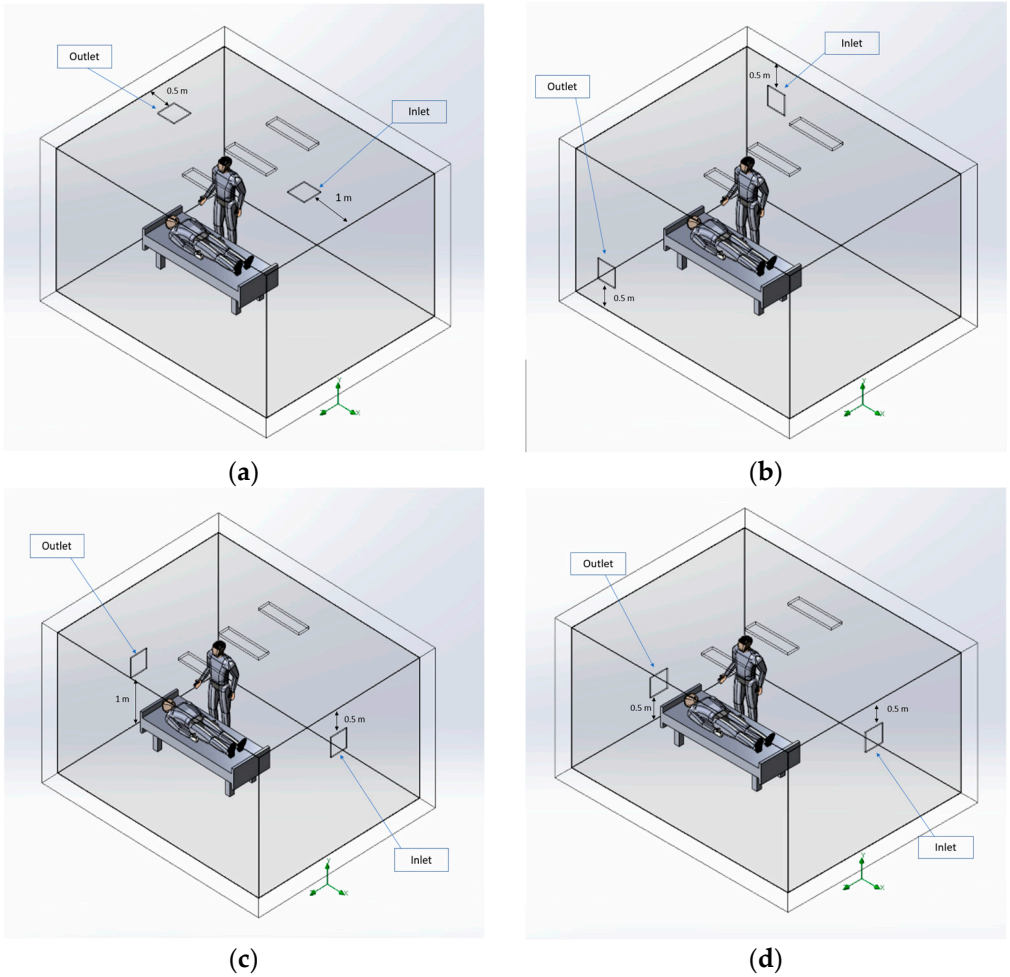

Figure 2. The layout of the isolation room with different diffuser locations (**a**) cases 1, 2, and 3; (**b**) cases 4, 5, and 5; (**c**) cases 7, 8, and 9; (**d**) cases 10, 11, and 12.

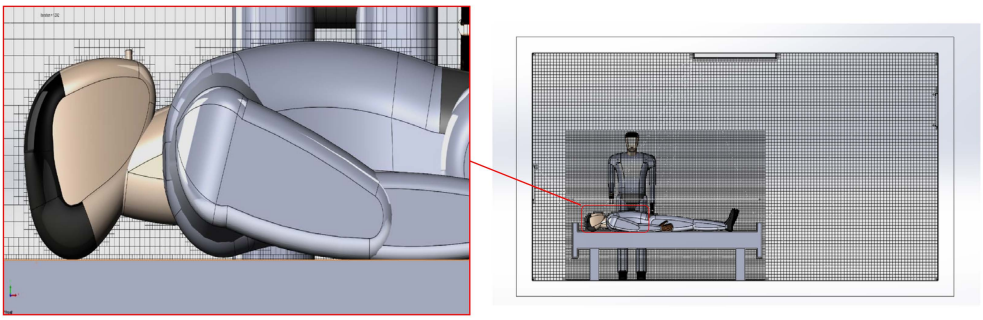

Figure 3. Domain meshes with zoom-in on the body edge.

The following input parameters [20] are shown in Table 1:

- Problem type (Internal, Compressible, 3D),
- Level of initial mesh (L_{ini}),
- Minimum gap size (h_{gap}) and minimum wall thickness (h_{wall}),
- Symmetry settings applied to the computational domain boundaries.

Table 1. Input parameters.

Parameter	Value
L_{ini}	From (3 to 7), respectively
h_{gap}	0.01 m
h_{wall}	0.01 m
y^+	10 mm [26]
Level of refining fluid cells	1
Level of refining cells at fluid/solid boundary	3

The mesh convergence study for grid independence analysis was conducted using five different mesh sizes, as illustrated in Table 2. A node was selected inside the domain (near the patient's mouth) to verify convergence, and a temperature gradient and velocity test was performed across the various refined meshes. As a result, the convergence error is reduced to less than 0.2% for temperature and 4% for velocity for the two finest meshes, as indicated in Figure 4. According to [27], it is acceptable to have a convergence error below 5%. When considering the precision, the processing power available, the domain's size, and the complexity of the curved surfaces, we chose the mesh with 2.46 M elements to run the simulations [28].

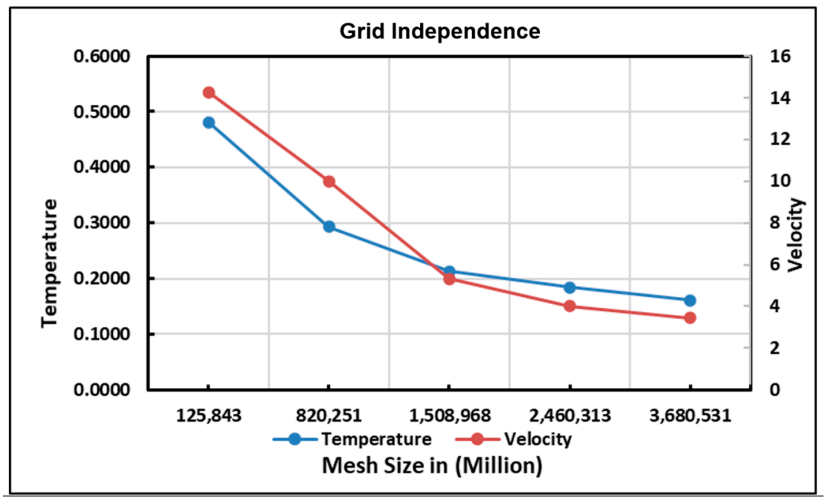

Figure 4. Temperature and air velocity percentage error at the control point vs. mesh size.

Table 2. Mesh sizes.

Mesh No.	Number of Elements
1	125,843
2	820,521
3	1,508,968
4	2,460,313
5	3,680,531

2.4. Boundary Conditions

Since boundary conditions are of primary significance in attaining desirable outcomes, it was essential to define them precisely. Hence, HVAC standards were reviewed, and a literature survey was done. The initial supply air velocity was kept at 9 ACH with no return air [19]. Afterward, the 12 and 15 ACH were applied. AIIRs (Airborne infectious isolation rooms) are designed following ASHRAE 170, an American standard [29]. The heat sources for both the healthcare worker and the patient are 144 W and 81 W, while the ceiling light is chosen to be 11 W. [29,30]. In addition, it is assumed that the walls are adiabatic, with no heat transfer or storage. Table 3 summarizes the remaining boundary conditions.

Table 3. Defined Boundaries.

	Type	Value
Room Air	Initial Temperature	289 K [29–31]
	Pressure	101,325 Pa
	Humidity	50%
	Turbulence Intensity	2%
	Turbulence Length	0.335 m
Supply Air	Volume Flow	0.14, 0.18, and 0.23 m^3/s
	Temperature	298 K
	Pressure	101,325 Pa [29–31]
	Humidity	50%
	Turbulence Intensity	20% [32]
	Turbulence Length	0.16 m
Expired Air	Mass Flow	0.00014 kg/s [29–31]
	Temperature	307 K
	Pressure	101,325 Pa
	Humidity	100% [31]
	Turbulence Intensity	2% [33]
	Turbulence Length	0.12 m [34]
Exhaust	Pressure	101,322.5 Pa

2.5. The Validation of the Numerical Solution

The numerical results were compared with experimental temperature room readings of a similar study [35]. The case study is an isolation room with the same airflow rate of 12 ACH and similar locations for the inlet and the outlet. Figure 5 demonstrates a vertical line next to the patient where the temperature values are taken. The CFD simulations compare well with the experimental temperature results, with a relative error of less than 1.09%, as shown in Figure 6 [5,36,37].

To further guarantee that the findings of PMV and PPD are reasonable, a validation based on two other parameters (temperature and velocity) has been presented for case 1. The average temperature in a public building is one factor that is considered by analysts when rating the facility's thermal comfort because the rate at which temperature affects thermal comfort varies [38]. From Figure 7, it can be seen the supply diffuser provides the space with airflow with a velocity around 1 m/s as illustrated by Figure 8. It's temperature about 298 K, and compared to case 1 as shown Figure 9, that corresponding to the 0 PMV

value, while the area above the bed covered by the range of temperature from 301 to 304 K, which match up with the results of PPD, where (60–100)% of people are not satisfied with the temperature in this region, as shown in Figure 10 case 1.

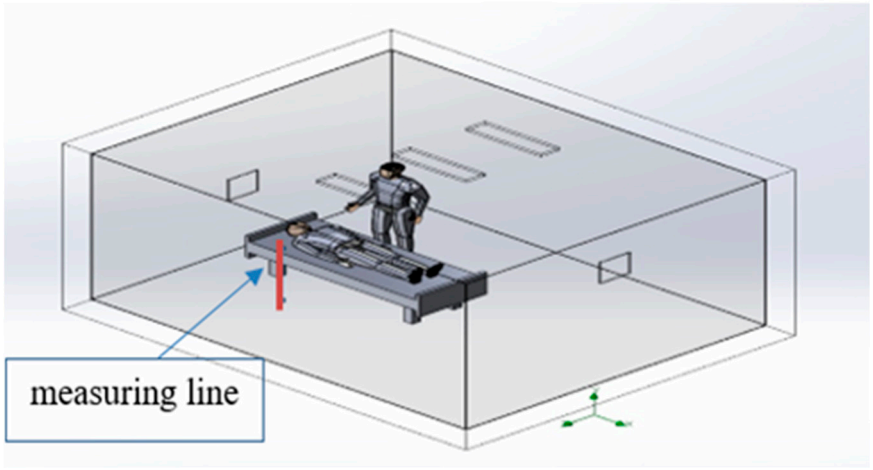

Figure 5. Illustration of the Position of the Measuring Line.

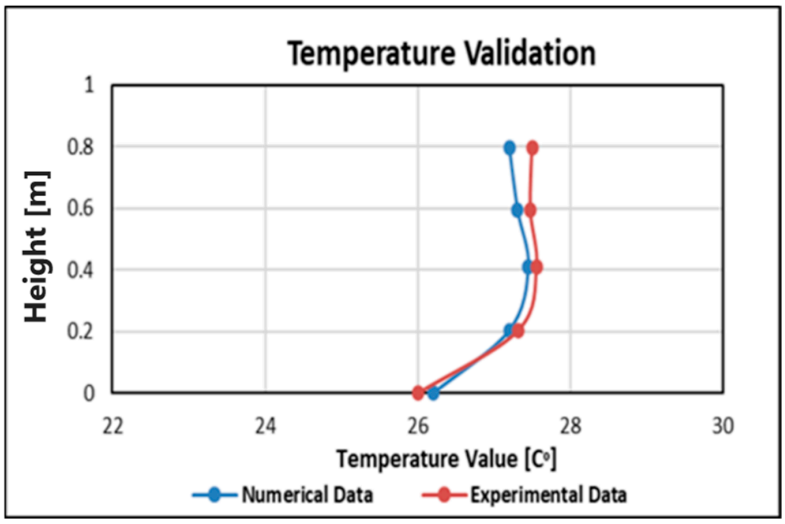

Figure 6. The Comparison with an Experimental Study.

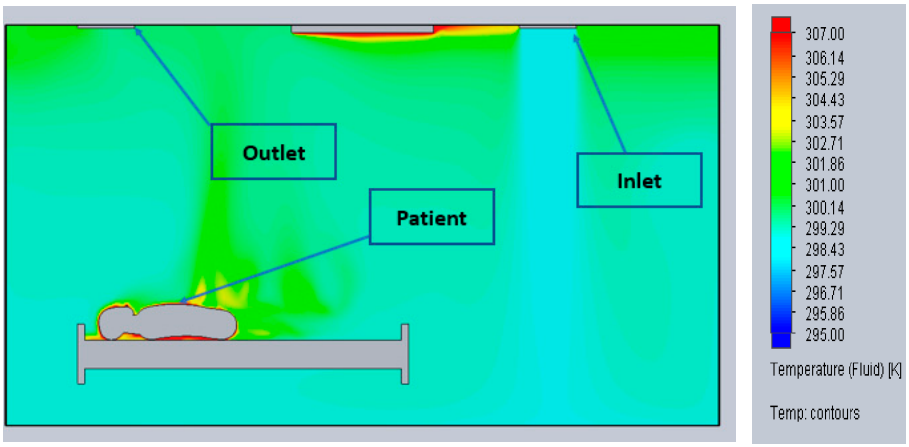

Figure 7. Front view for Temperature Case 1 at 9 ACH.

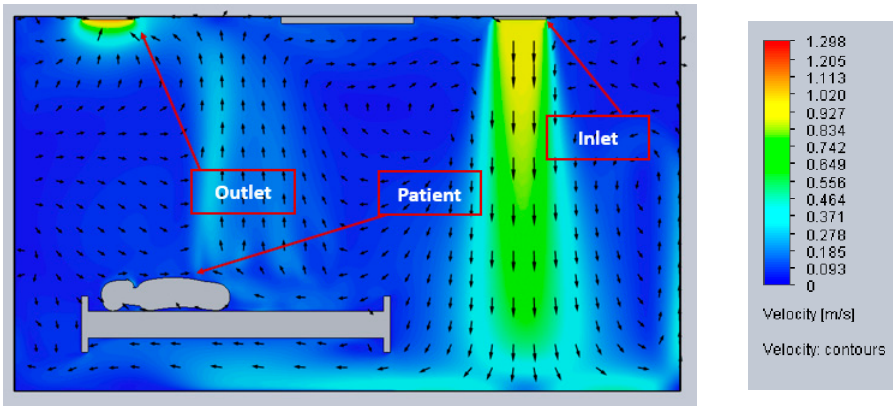

Figure 8. Front view for Velocity Case 1 at 9 ACH.

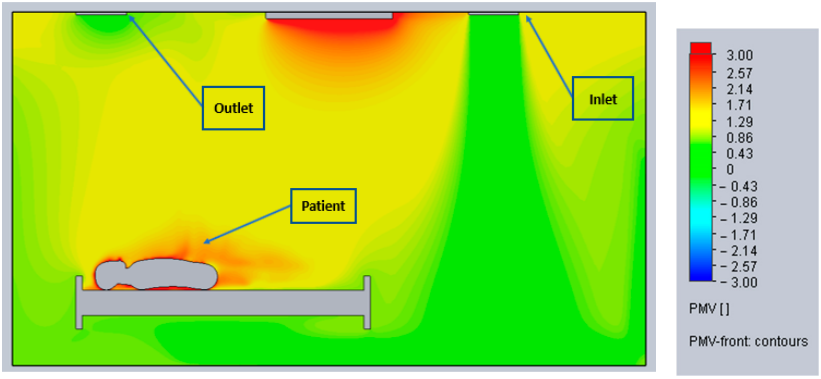

(**a**)

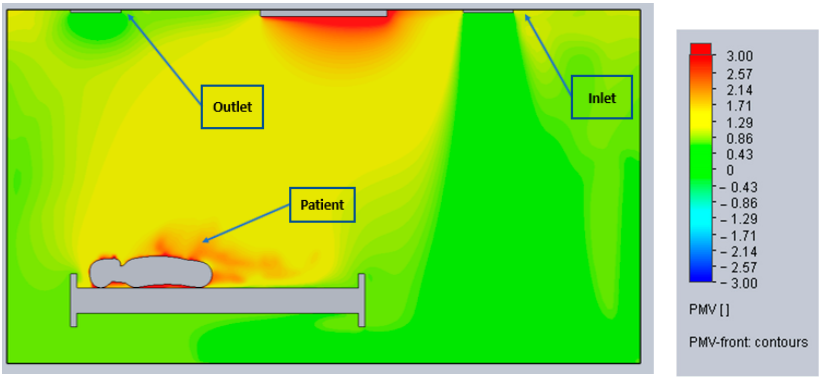

(**b**)

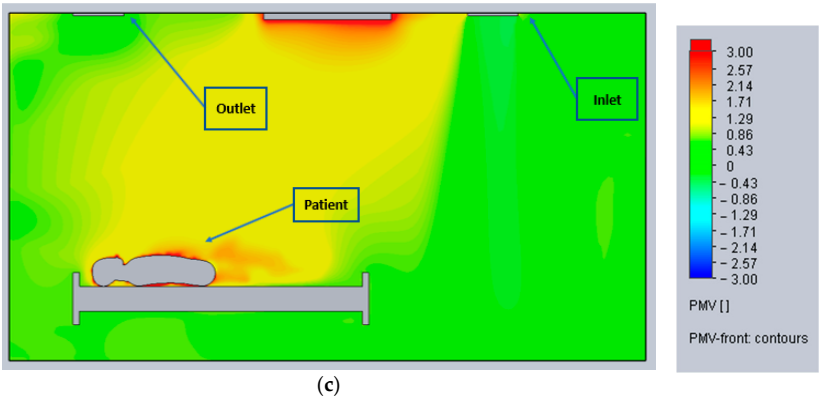

(**c**)

Figure 9. Front view for PMV (**a**) Case 1 at 9 ACH, (**b**) Case 2 at 12 ACH, (**c**) Case 3 at 15 ACH.

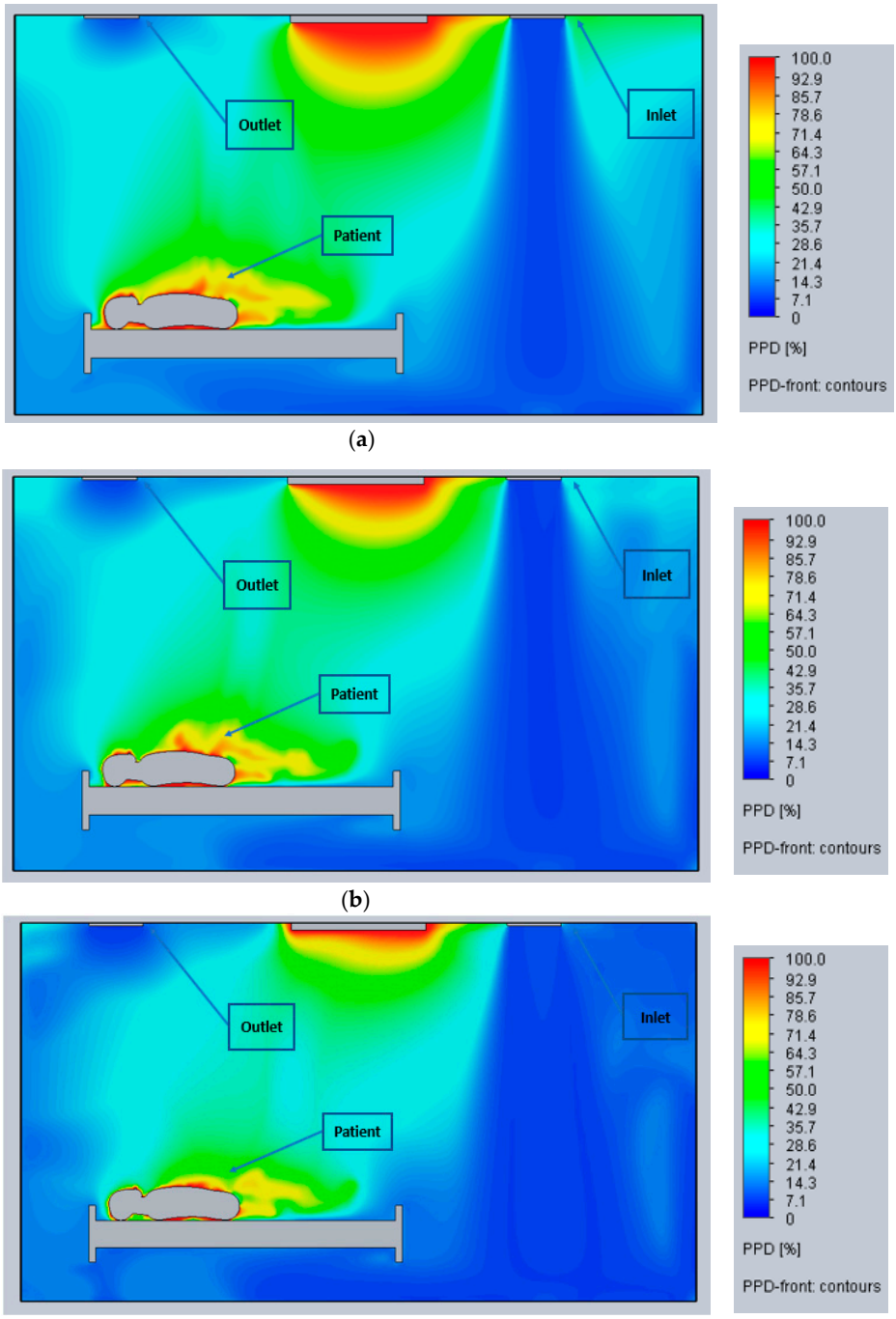

Figure 10. Front view for Fluid PPD (**a**) Case 1 at 9 ACH, (**b**) Case 2 at 12 ACH, (**c**) Case 3 at 15 ACH.

Meanwhile, the velocity result shows that adequate velocity is the foundation for thermal comfort (within the permitted velocity range) as shown in Figure 8 [36], and this is proved in both Figures 9 and 10 (case 1).

3. Results and Discussion

This section compares the most representative simulation results for the various geometries and airflow configurations regarding thermal comfort indicators. The results will include PPD and PMV to assess thermal comfort and ADPI for airflow diffusion. The results were visualized using the front and top section views. It can be noticed from Figure 2 that designs (a) and (b) exhibit distinct differences. In contrast, Figure 2 designs (c) and (d) show a high degree of similarity, which emphasizes the effect of the diffuser's level on

thermal comfort. It justifies the necessity to simulate all of the 12 cases to comprehensively assess the impact of each design on thermal comfort.

3.1. Cases 1, 2, and 3

As shown in Figure 2a, the inlet and outlet of this design are roof-mounted, at 1 m for the inlet and 0.5 m for the outlet from the side wall.

3.1.1. Predicted Mean Vote (PMV)

Figure 9a depicts the front view for an airflow of 9 ACH, with the green zone covering the area below the patient level around 0 PMV. Going up, the value of PMV gradually increases until it reaches approximately 1.3 PMV, where the feeling of warmth is dominant owing to the buoyancy factor. Similar results are observed with 12 ACH airflow (Figure 6) but with a more extended green area due to the increased airflow. The warmth area gradually declines in the occupied zone. Therefore, an increase in airflow improves thermal comfort. However, at 15 ACH (Figure 9c), the upper region is still thermally uncomfortable as the airflow is not directed toward, and cannot reach, that area. In addition, due to the inlet location, as seen in Figure 9a–c, the whole region under the inlet is at PMV = 0.

3.1.2. Predicted Percent Dissatisfied (PPD)

Temperature plays a crucial role in characterizing PPD, and dissatisfaction in this area leads to results consistent with the thermal prediction (PMV). As seen in Figure 10a, at 9 ACH, the thermal comfort is best achieved below the inlet (about 0% PPD) inside the suggested range of 0–7% PPD suggested by [37]. In contrast, thermal discomfort starts outside the air path, going up over the patient's body. Especially in the space where the patient and the HCW are located, the predominant value is 50% PPD, which is considered high [6,37]. It is because the bed works as a barrier preventing the air from reaching the upper region, dispersing the air to the sides. For 12 and 15 ACH (Figure 10b,c), thermal discomfort decreases on the inlet side, a slight improvement. However, the occupied area is still not affected by the higher airflow, and the predominant values are from 30–50% PPD in this region.

3.2. Cases 4, 5, and 6

The inlet is behind the HCW at 0.5 m below the ceiling in these cases. The outlet is on the opposite wall, 0.5 m above the floor, as shown in Figure 2b.

3.2.1. Predicted Mean Vote (PMV)

Figures 11a and 12c results correspond to 9 ACH airflow. The predominant feeling is warmth, with a value of about 1.29 PMV. Higher values, 2 to 3 PMV, are observed in the occupied area because of body heat. Normal thermal conditions occur in the room beside the wall on the side of the patient's head and the airflow path. In addition, we notice the green space at the lower level beside the bed due to the backflow from the wall (Figure 12a). At 12 ACH (Figures 11b and 12b), the comfort zone (green) increases primarily near the room walls with values from 0–0.8 PMV. As air hits the opposite wall, it spreads gradually toward the center. Furthermore, Figure 11c shows that the green area has increased due to the increase in airflow, despite some hot spots near the ceiling, with values from 1–2 PMV.

Raising the airflow to 15 ACH reduces the warm and hot regions except for the corner above the inlet, where the PMV ranges between 0.9 and 1.7 PMV (Figures 11b and 12b). However, the occupied area is again suffering from the warmth, as is evident from the top view in Figure 11c. This is because the inlet is higher than the occupancy level, pushing the air toward the opposite side.

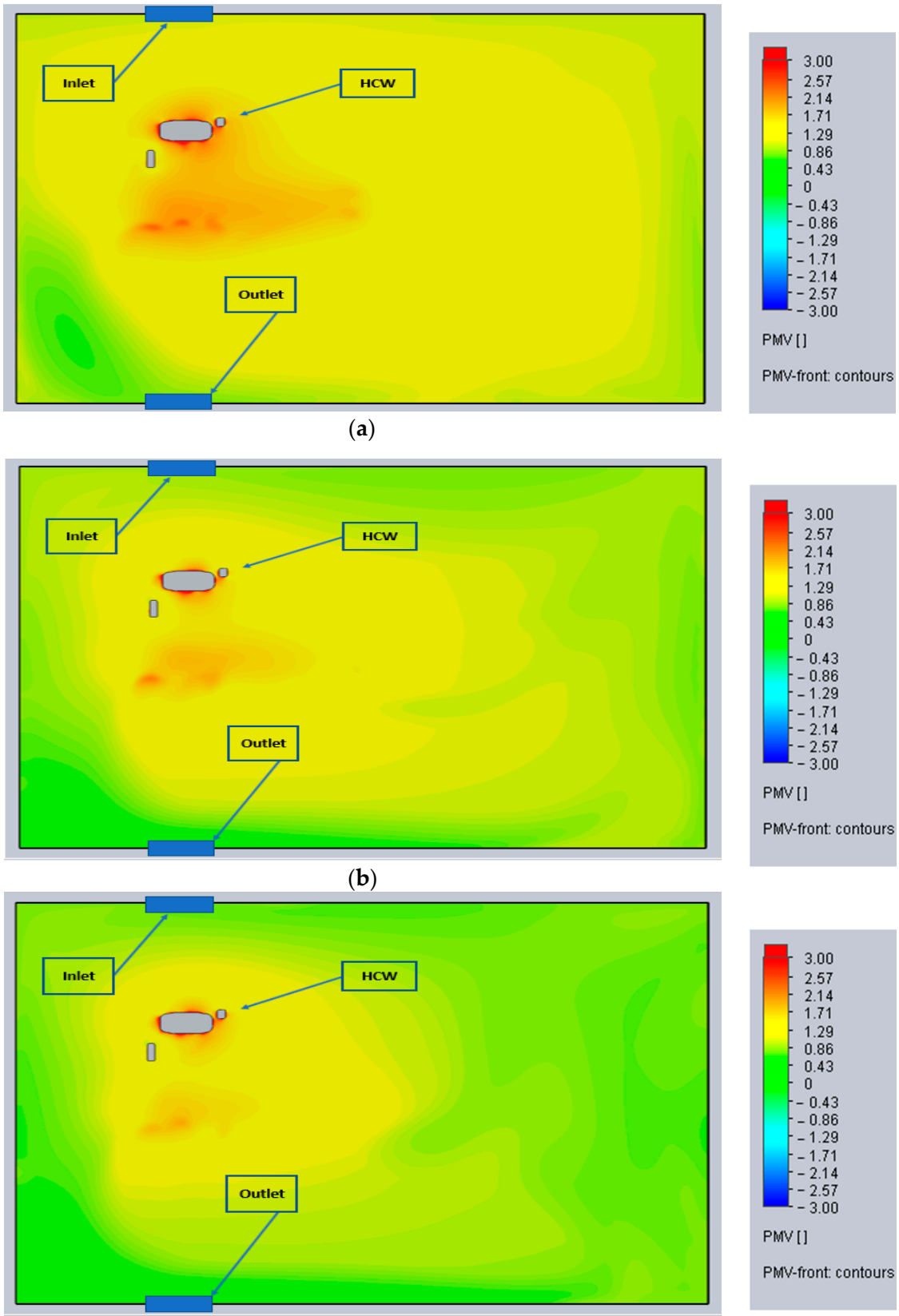

Figure 11. Top view (**a**) Case 4 at 9 ACH, (**b**) Case 5 at 12 ACH, (**c**) Case 6 at 15 ACH.

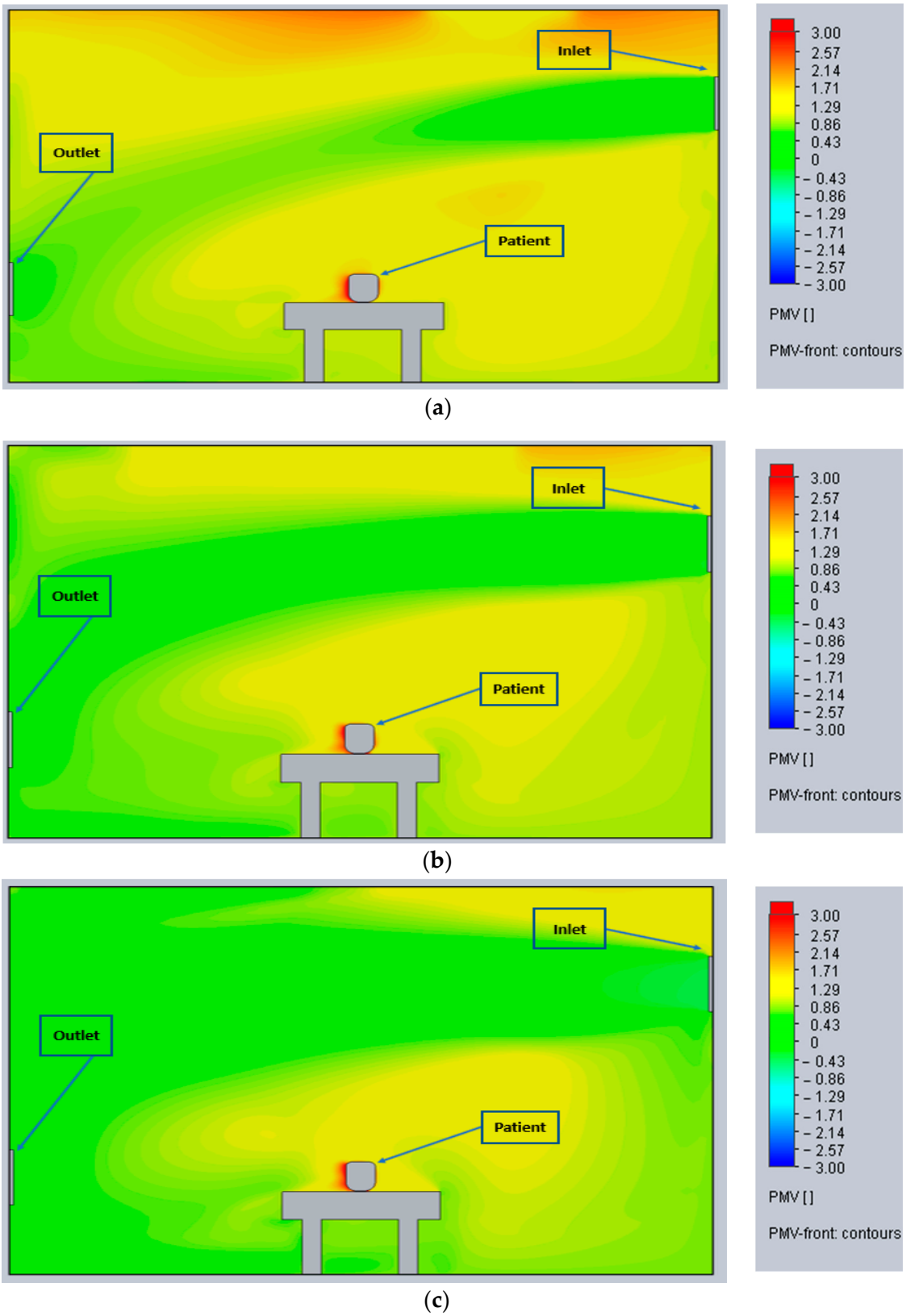

Figure 12. Front view for PMV (**a**) Case 4, at 9 ACH, (**b**) Case 5 at 12 ACH, (**c**) Case 6 at 15 ACH.

3.2.2. Predicted Percent Dissatisfied (PPD)

Figure 13a, at 9 ACH, shows that the occupied place has a value of more than 43% PPD. This number is characteristic of a considerable portion of the room and diminishes as

airflow speed increases. The PMV value decreases to 28% PPD and below in the regions near the walls. Figure 13b,c, for 12 and 15 ACH, shows that the occupied area has a value starting at 20–25% PPD and goes up far from the inlet effect. At the same time, the PPD is lower near the room walls. Furthermore, the increase in airflow decreases the value of PPD from the borders to the center of the room where the occupied area is, as shown in Figure 13b,c.

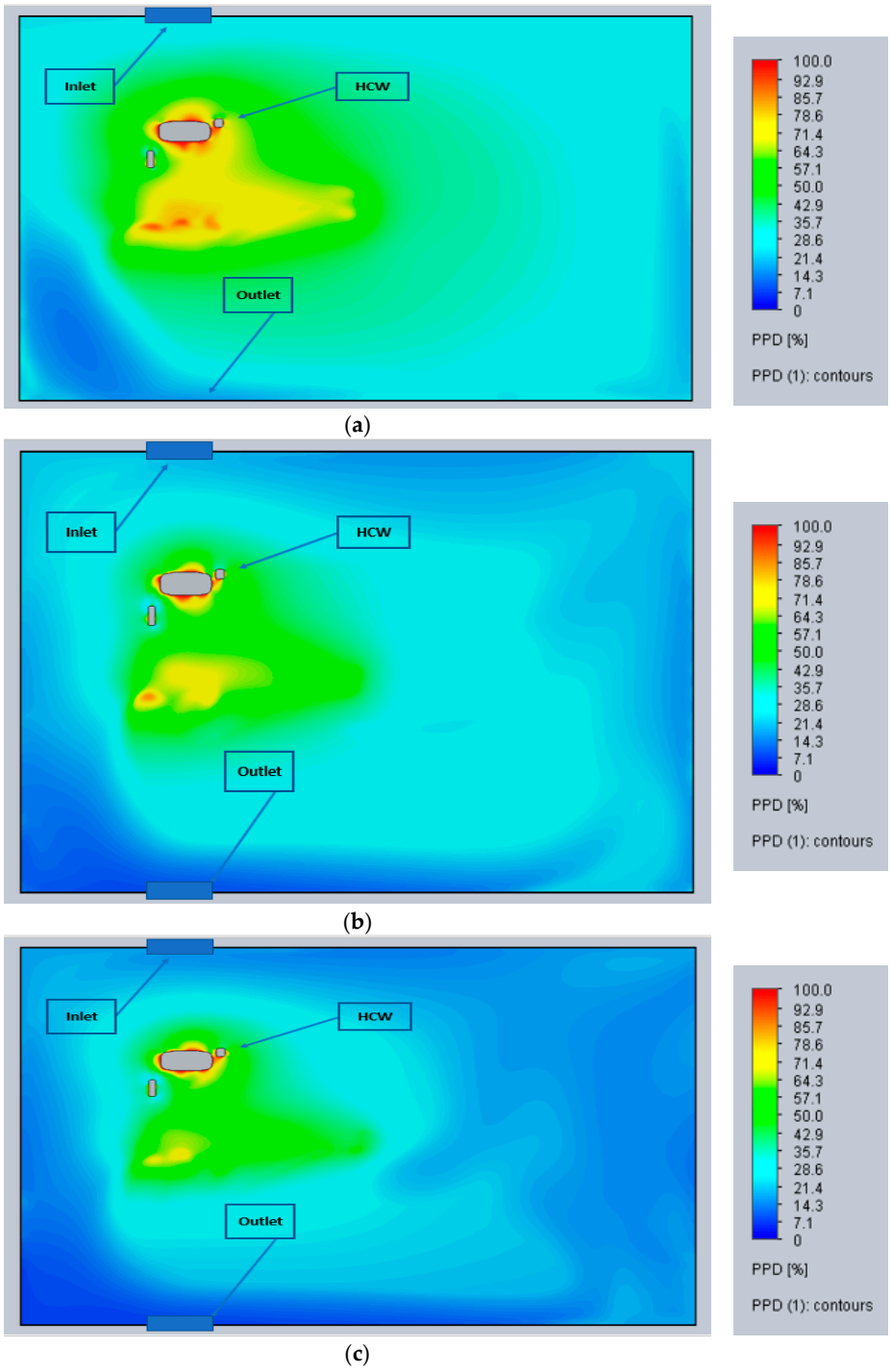

Figure 13. Top view for Fluid PPD (**a**) Case 4 at 9 ACH, (**b**) Case 5 at 12 ACH, (**c**) Case 6 at 15 ACH.

3.3. Cases 7, 8, and 9

The inlet is 0.5 m from the ceiling on the patient's feet wall, while the outlet is 1 m above the floor on the opposite wall, as shown in Figure 2c.

3.3.1. Predicted Mean Vote (PMV)

Figure 14 shows the thermal balance illustrated by PMV values. At 9 ACH, the majority of the area in yellow in Figure 14a is around 1.29 PMV, indicating a warm zone. The airflow follows the green zone at about 0 PMV, characterized by a feeling of thermal comfort. This is not the case for the upper region (in red), where the value is 3 PMV. The temperature is higher due to the hot air's buoyancy and the lights' thermal load. The green area is expanded for 12 ACH (Figure 10b) due to increased airflow. The influence of the airflow on PMV is more significant at 15 ACH (Figure 14c), where most of the region is green (0 PMV). A green area indicates neutral feelings up to the higher level, the only exceptions being some regions around the occupied area. The occupied zone is yellow and red near the patient, with values between (1.3 and 3) PMV. Due to the horizontal flow pattern, air will not pass through the occupied area, accumulating heat.

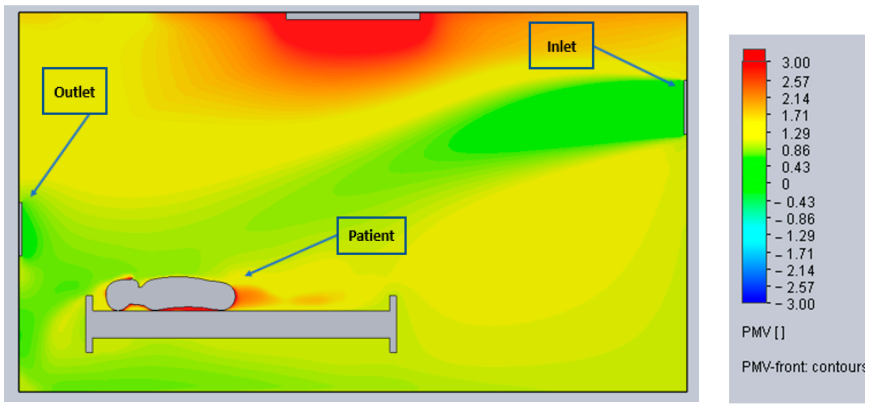

(**a**)

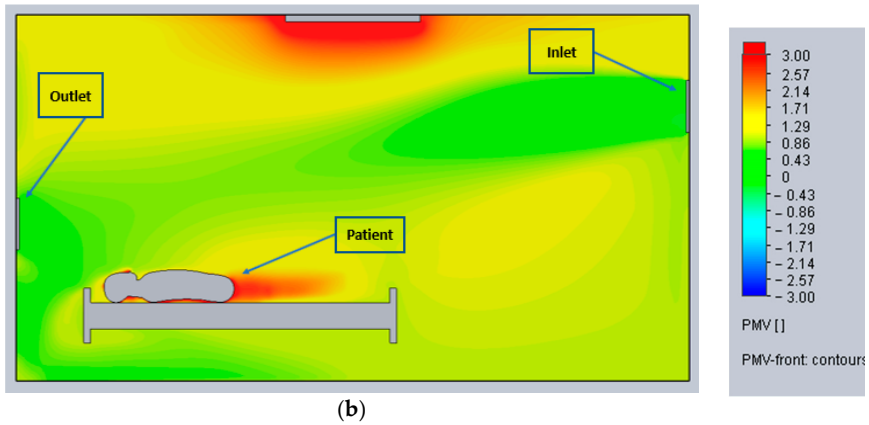

(**b**)

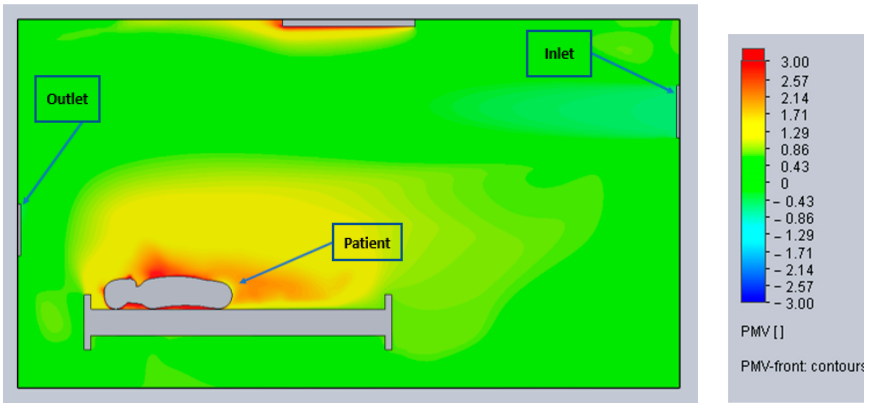

(**c**)

Figure 14. Front view for PMV (**a**) Case 7 at 9 ACH, (**b**) Case 8 at 12 ACH, (**c**) Case 9 at 15 ACH.

3.3.2. Predicted Percent Dissatisfied (PPD)

The ideal value is 0 for the PPD, indicating that everyone is comfortable with the environment's temperature. However, we see in Figure 15a,b, for 9 AFC and 12 AFC, respectively, that most of the room space has a PPD value starting at 25% PPD. However, due to airflow passage, PPD is less than 25% in the occupied zone. Furthermore, for 15 ACH (Figure 15c), the value is from 0–7% PPD, which corresponds to the value suggested by [37], which should not exceed 10% PPD. In this case, however, the occupied area is penalized by the strong horizontal airflow pattern and has a high PPD value of 30% or more. This indicates that a rise in airflow positively affects thermal comfort only if appropriately diffused.

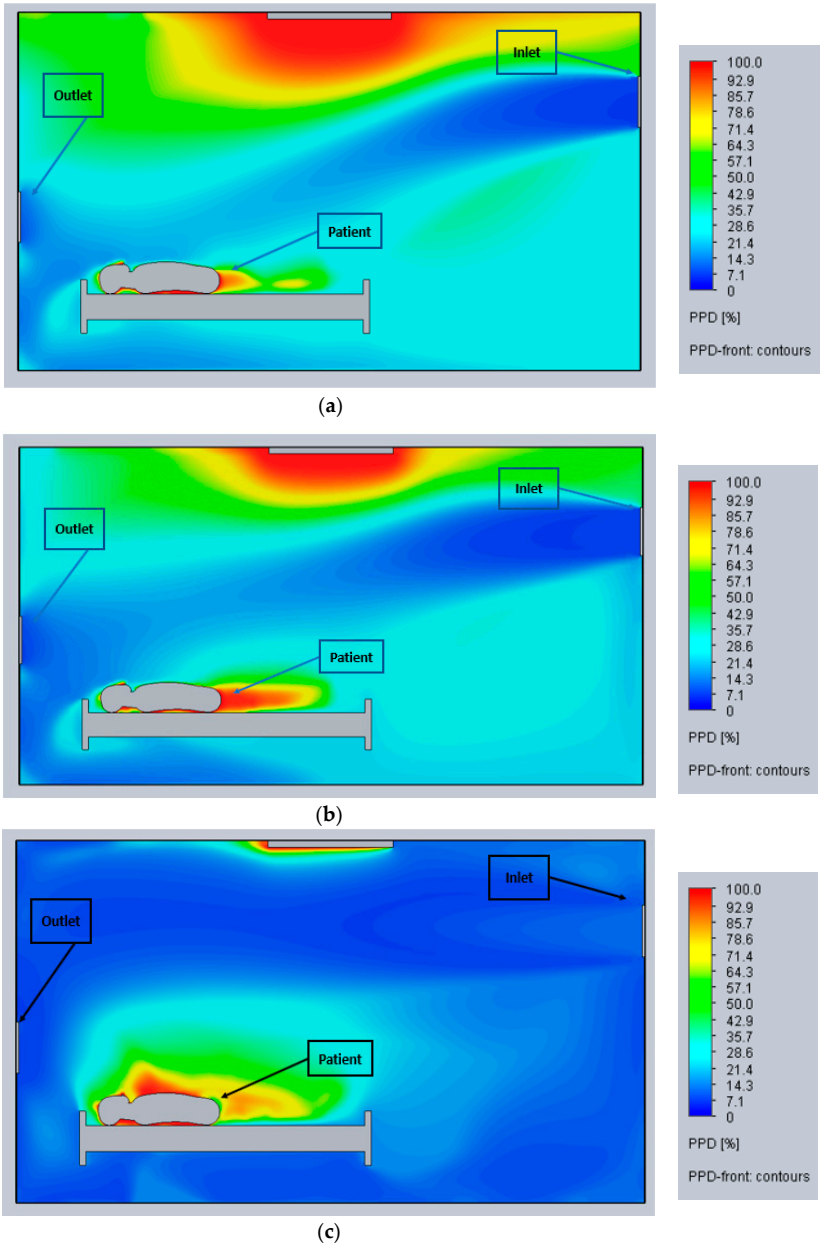

Figure 15. Front view of PPD (**a**) Case 7 at 9 ACH, (**b**) Case 8 at 12 ACH, (**c**) Case 9 at 15 ACH.

3.4. Cases 10, 11, and 12

These test cases have an almost identical geometry to the previous ones, except the outlet is situated only 0.5 m from the floor, as seen in Figure 2d.

3.4.1. Predicted Mean Vote (PMV)

For 9 ACH (Figure 16a), the green area is concentrated above the occupied region because the airflow path reaches up to the patient's line, where the value of PMV is around 0. In addition, the outlet absorbs the air directly, which does not allow the air to move around the room, leading to thermal discomfort elsewhere, with PMV values around 1.3. At 12 ACH (Figure 16b), the green area increases significantly throughout the room, with the predominant PMV values between 0 and 0.8 due to increased airflow. Moreover, the value of PMV gradually rises in the patient's area, which means a more uncomfortable feeling because the supplied air tends to become parallel to the patient, with values starting at 1.3 PMV and more. The upper area has good thermal comfort values for 15 ACH with PMV around 0, except for the region surrounding the light (Figure 16c). However, at 15 ACH, the bed area has an undesirable PMV value because the strong airflow results in a horizontal pattern.

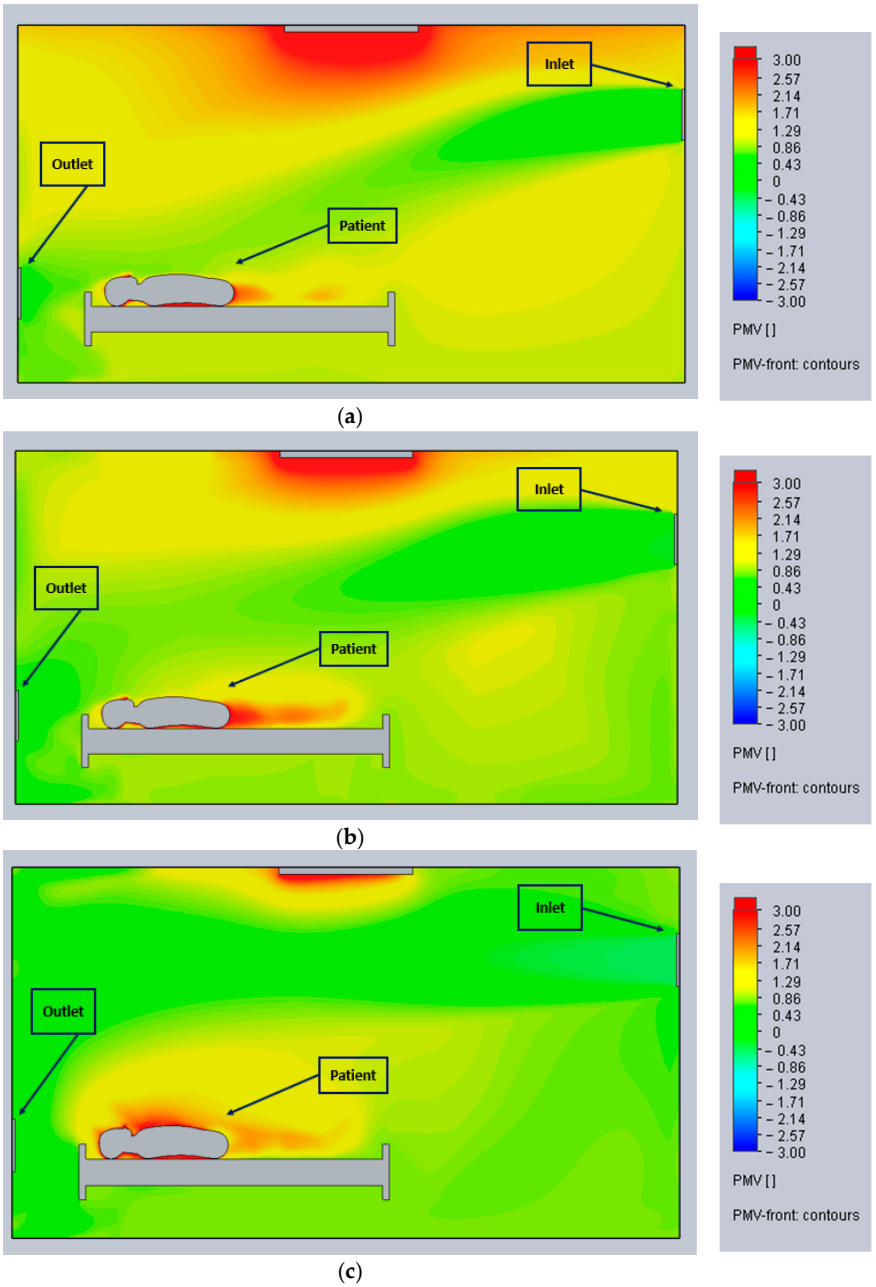

Figure 16. Front view for PMV (**a**) Case 10 at 9 ACH, (**b**) Case 11 at 12 ACH, (**c**) Case 12 at 15 ACH.

3.4.2. Predicted Percent Dissatisfied (PPD)

By repositioning the outlet, the outcomes are similar to the results in cases 7, 8, and 9, according to the simulation results. In this design (Figure 2d), for 9 ACH (Figure 17a), the only variance is the level of thermal satisfaction, which decreases near the ground due to the location of the outlet. At 12 ACH (Figure 17b), we notice an expansion of the thermal satisfaction area. Throwing the air with more force causes the path to become horizontal instead of going downwards because of gravity, which increases exchanges. At 15 ACH (Figure 17c), there are similarities with case 9 (Figure 15c) due to the strength of the flow. Moreover, there is no significant effect of the outlet's location between these two designs (Figure 2c,d).

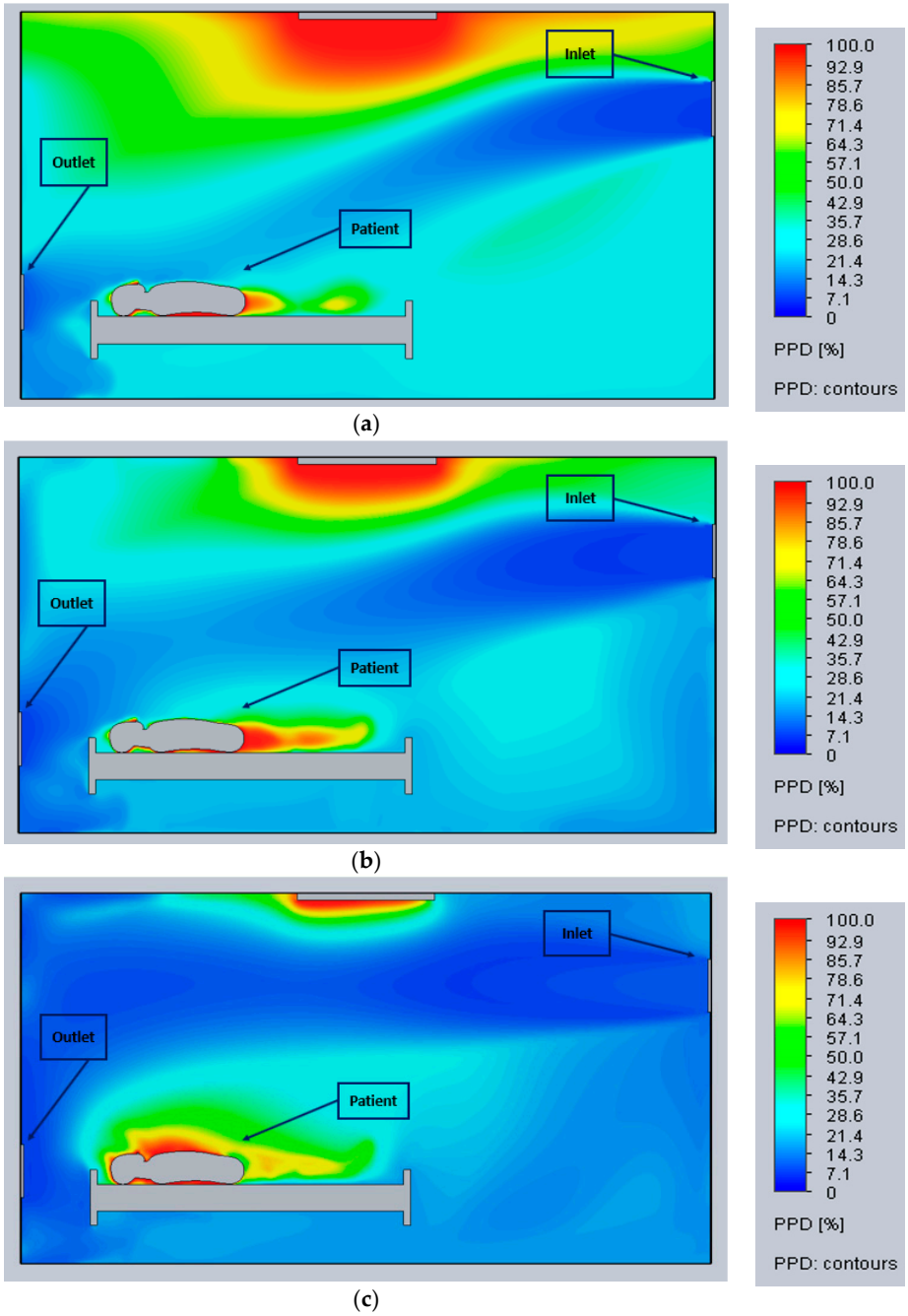

Figure 17. Front view for Fluid PPD (**a**) Case 10 at 9 ACH, (**b**) Case 11 at 12 ACH, (**c**) Case 12 at 15 ACH.

3.5. PPD Variation along the Measuring Line

The charts will display the parameter variation along a line drawn at a vertical distance of 1 m from the ground and parallel to the patient over a distance of 2 m, as shown from Figure 18. This section analyzes the PPD variation along this measuring line, a representative measure of the comfort level in the occupied zone of the room. For example, it shows the PPD variation for an airflow of 9 ACH. We notice (Figure 19—cases 7 and 10) that the designs shown in Figure 2c,d have the best thermal comfort with PPD values between 18 and 30%. At 12 ACH (Figure 20—cases 8 and 11), a similar behavior is observed, with some values of PPD for case 8 of more than 30%. It is worth mentioning that these optimal designs have been suggested by [25]. However, for 15 ACH (Figure 21), it has been found that all PPD values are too high, as the strong horizontal airflow does not cross the occupied area. In conclusion, Figures 19 and 21 demonstrate that a higher Air Changes per Hour (ACH) value significantly enhances thermal comfort. Additionally, the location of the diffuser plays a crucial role, as evidenced by designs (a) and (b) shown in Figure 2 which present optimal values for the PPD and, consequently, the PMV.

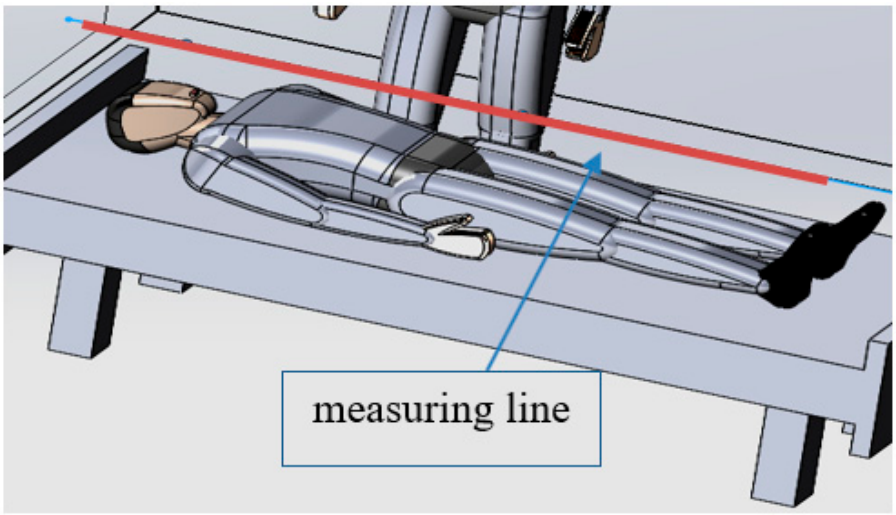

Figure 18. Illustration of the position of the measuring line.

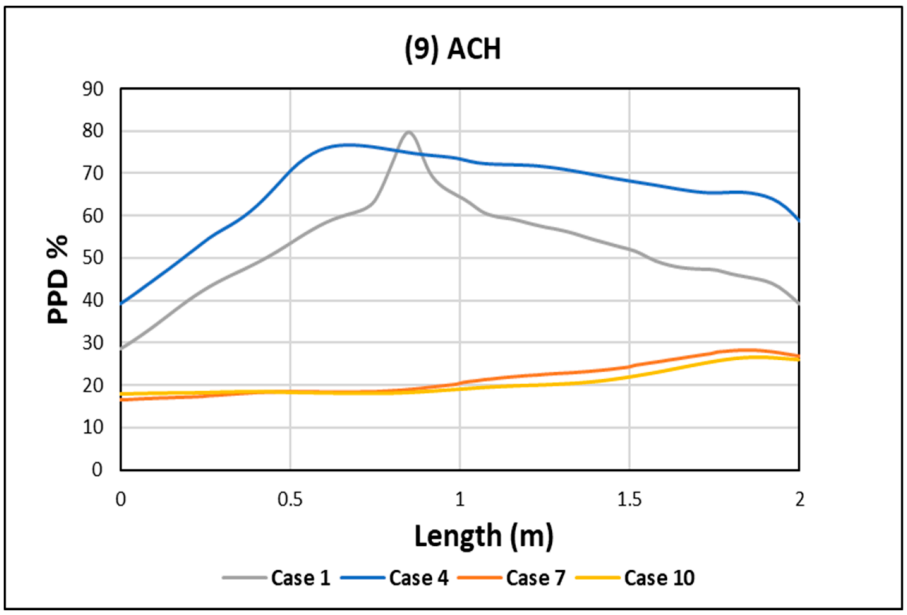

Figure 19. Comparison of PPD % at 9 ACH.

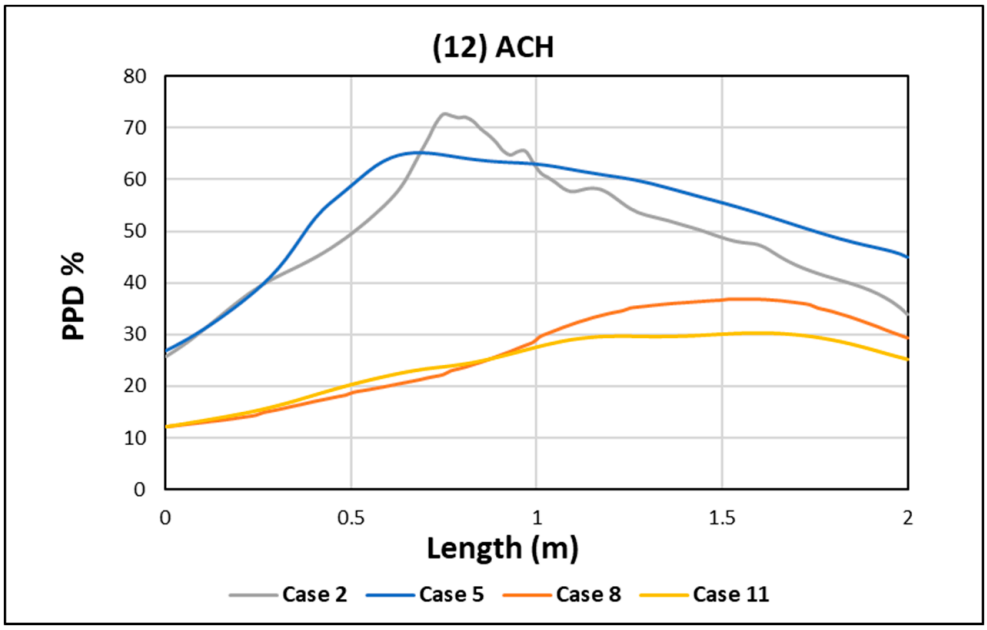

Figure 20. Comparison of PPD % at 12 ACH.

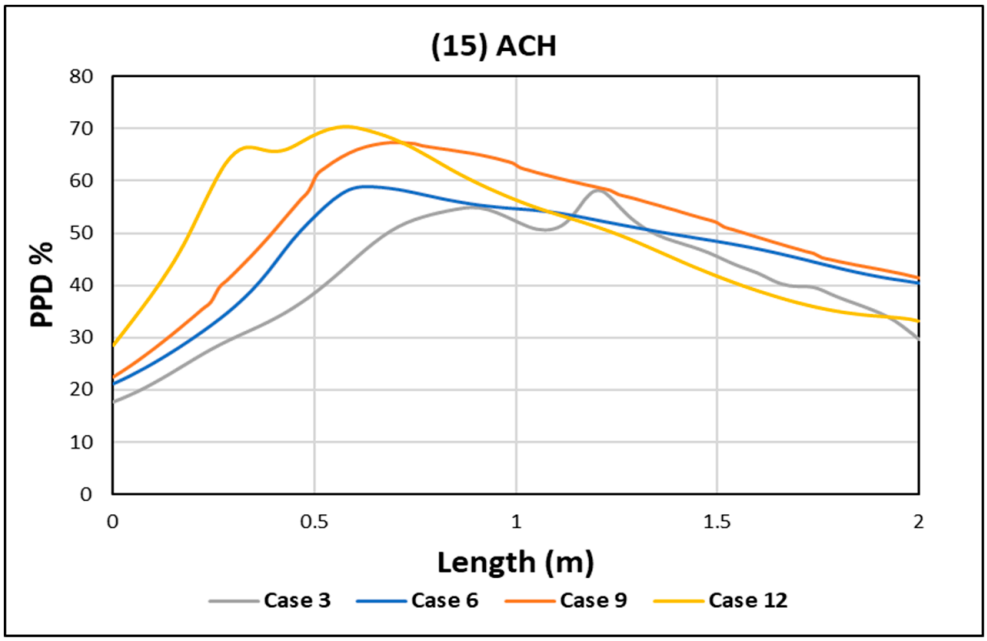

Figure 21. Comparison of PPD % at 15 ACH.

3.6. Air Diffusion Performance Index (ADPI)

The ADPI values reveal the achieved percentage of air diffusion in each case. Case 6 is the optimum one, as the value is more than 80%, the lower limit for thermal comfort, according to [39]. As shown in the chart (Figure 22), the efficiency of air diffusion shows how the values gradually increase with the airflow. Generally, for 15 ACH, all the cases are acceptable. For 12 ACH, reasonable outcomes were achieved, except for case 2, which was lower than the 80% ADPI limit. This result indicates the effect of airflow and diffuser location on the outcomes. At 9 ACH, all designs failed to meet the minimal requirement for ADPI.

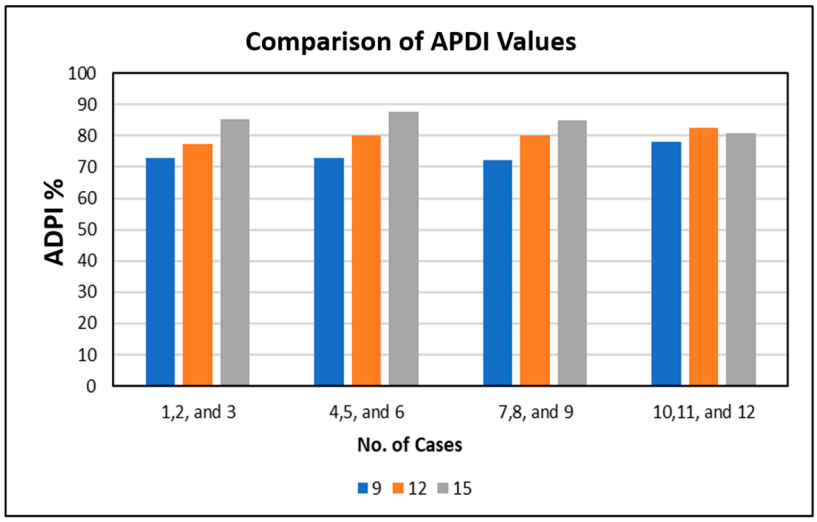

Figure 22. Comparison of ADPI Values.

In our current investigation, we observed distinct trends in thermal comfort that contrast and expand upon our previous findings on contaminant removal [18] Notably, while our earlier study highlighted the critical role of diffuser placement in effective contaminant extraction, the current results reveal a more complex interaction between diffuser location and thermal comfort parameters like PMV and PPD. These findings suggest that optimizing air quality does not inherently guarantee thermal comfort, underscoring the need for a balanced HVAC system design for healthcare settings.

4. Conclusions

The importance of ventilation to human health and its impact on thermal comfort in hospital environments prompted our study on the ventilation configurations of a hospital room. Thermal comfort parameters were evaluated within various ventilation designs and airflow rates using CFD simulations. More specifically, the influence of the inlet/outlet locations on the thermal comfort parameters has been studied.

Our findings indicate a notable impact of diffuser location and airflow intensity on thermal comfort. However, not all designs achieved an ideal thermal environment, with the most effective being cases 7 and 10 at 9 ACH. These cases demonstrated targeted thermal comfort in the patient area due to the strategic placement of the air outlet and inlet.

Furthermore, our results underline the considerable influence of airflow on the air diffusion performance index (ADPI), with higher ACH designs showing better air diffusion, (even though although achieving complete thermal comfort remained challenging for specific scenarios). It deserves to be mentioned that designs (a) and (b) can be chosen for a lower value of ACH, where design (b) has a better value of about 10% PPD of design (a) at 9 and 12 ACH. In contrast, designs (c) and (d) have low down values by about 40%. At 15 ACH, we found that PPD has a high value over the patient's area in the four designs.

The results show that the airflow or the inlet/outlet location alone do not provide optimum thermal comfort. Although many studies have been conducted in this area, much effort is needed to optimize the designs by adding blades to the diffusers, and the study could be transient instead of steady state. In addition, some challenges to overcome during the modeling process include the model's size. Therefore, further simulations are recommended for other designs.

Building upon our previous work, this study sheds light on previously unexplored aspects, revealing that optimal thermal comfort transcends mere airflow or diffuser location. This goes against what is commonly believed in this regard and opens avenues for future research, including exploring transient models and incorporating adjustable diffusers. Such advancements promise to deepen our understanding and contribute to more effective, patient-centered HVAC solutions in healthcare facilities.

Despite the abundance of literature in this area, extensive effort remains required to uncover effective designs. However, there are still a lot of obstacles to overcome while modeling, like the model's size. In addition to modeling, the experimental work will confirm the results. When it comes to thermal comfort or pollutant removal efficiency, employing diffusers angled at a specific angle is also essential, which can be implemented in future studies.

Author Contributions: Conceptualization, M.A.; methodology, M.A.; software, M.A.; validation, M.A.; formal analysis, M.A.; investigation, M.A.; resources, M.A.; data curation, M.A.; writing—original draft preparation, M.A. and A.I.; writing—review and editing, M.A., A.I., F.M. and M.Y.H.; visualization, M.A.; supervision, A.I., F.M. and M.Y.H.; project administration, A.I. and M.Y.H.; funding acquisition, A.I. All authors have read and agreed to the published version of the manuscript.

Funding: The authors kindly acknowledge the financial contribution from the Natural Sciences and Engineering Research Council—NSERC Canada, through a discovery research grant.

Data Availability Statement: The detailed data and simulations reported in the paper are available upon mail request from the authors.

Conflicts of Interest: The authors declare no conflicts of interest.

References

1. Alotaibi, B.S.; Lo, S.; Southwood, E.; Coley, D. Evaluating the Suitability of Standard Thermal Comfort Approaches for Hospital Patients in Air-Conditioned Environments in Hot Climates. *Build Environ.* **2020**, *169*, 106561. [CrossRef]
2. Bouzidi, Y.; El Akili, Z.; Gademer, A.; Tazi, N.; Chahboun, A. How Can We Adapt Thermal Comfort for Disabled Patients? A Case Study of French Healthcare Buildings in Summer. *Energies* **2021**, *14*, 4530. [CrossRef]
3. El akili, Z.; Bouzidi, Y.; Merabtine, A.; Polidori, G.; Kauffmann, J. Assessment of Thermal Comfort of Frail People in a Sitting Posture under Non-Uniform Conditions Using a Thermal Manikin. *Build. Environ.* **2022**, *221*, 4530. [CrossRef]
4. Rad, H.R.; Khodaee, Z.; Ghiai, M.M.; Arjmand, J.T.; El Haj Assad, M. The Quantitative Assessment of the Effects of the Morphology of Urban Complexes on the Thermal Comfort Using the PMV/PPD Model (a Case Study of Gheytariyeh Neighborhood in Tehran). *Int. J. Low Carbon Technol.* **2021**, *16*, 672–682. [CrossRef]
5. *HVAC Design Manual for Hospitals and Clinics*; American Society of Heating, Refrigerating and Air-Conditioning Engineers: Atlanta, GA, USA, 2013; ISBN 9781936504398.
6. *ANSI/ASHRAE Standard 55-2004; Thermal Environmental Conditions for Human Occupancy. ASHRAE Standard: Atlanta, GA, USA,* 2004.
7. Mohamed Kamar, H.; Kamsah, N.B.; Ghaleb, F.A.; Idrus Alhamid, M. Enhancement of Thermal Comfort in a Large Space Building. *Alex. Eng. J.* **2019**, *58*, 49–65. [CrossRef]
8. Price Engineer's HVAC Handbook. Engineering Guide Air Distribution. 2011. Available online: https://www.priceindustries.com/content/uploads/assets/literature/engineering-guides/air-distribution-engineering-guide.pdf (accessed on 5 March 2023).
9. Borowski, M.; Łuczak, R.; Halibart, J.; Zwolińska, K.; Karch, M. Airflow Fluctuation from Linear Diffusers in an Office Building. The Thermal Comfort Analysis. *Energies* **2021**, *14*, 4808. [CrossRef]
10. Chen, Z.; Xin, J.; Liu, P. Air Quality and Thermal Comfort Analysis of Kitchen Environment with CFD Simulation and Experimental Calibration. *Build. Environ.* **2020**, *172*, 106691. [CrossRef]
11. Prabhakaran, R.T.D.; Curling, S.F.; Spear, M.; Ormondroyd, G.A. Simulation model to evaluate human comfort factors for an office in a building. *Proceedings* **2018**, *2*, 1126.
12. Kainaga, T.; Sagisaka, K.; Yamada, R.; Nakaya, T. A Case Study of a Nursing Home in Nagano, Japan: Field Survey on Thermal Comfort and Building Energy Simulation for Future Climate Change. *Energies* **2022**, *15*, 936. [CrossRef]
13. Hwang, R.L.; Cheng, M.J.; Lin, T.P.; Ho, M.C. Thermal Perceptions, General Adaptation Methods and Occupant's Idea about the Trade-off between Thermal Comfort and Energy Saving in Hot-Humid Regions. *Build Environ.* **2009**, *44*, 1128–1134. [CrossRef]
14. van Gaever, R.; Jacobs, V.A.; Diltoer, M.; Peeters, L.; Vanlanduit, S. Thermal Comfort of the Surgical Staff in the Operating Room. *Build Environ.* **2014**, *81*, 37–41. [CrossRef]
15. Saadeddin, K.A.R. The Effects of Diffuser Exit Velocity and Distance between Supply and Return Apertures on the Efficiency of an air Distribution System in an Office Space. Master's Thesis, South Dakota State University, Brookings, SD, USA, 2016.
16. Cheng, Y.; Lin, Z.; Fong, A.M.L. Effects of Temperature and Supply Airflow Rate on Thermal Comfort in a Stratum-Ventilated Room. *Build Environ.* **2015**, *92*, 269–277. [CrossRef]
17. Bolashikov, Z.D.; Melikov, A.K.; Brand, M. General Rights Reduced Exposure to Coughed Air by a Novel Ventilation Method for Hospital Patient Rooms Reduced Exposure to Coughed Air by a Novel Ventilation Method for Hospital Patient Rooms; APA. 2012. Available online: https://core.ac.uk/download/pdf/43245643.pdf (accessed on 24 June 2022).
18. Alkhalaf, M.; Ilinca, A.; Hayyani, M.Y. CFD Investigation of Ventilation Strategies to Remove Contaminants from a Hospital Room. *Designs* **2023**, *7*, 5. [CrossRef]

19. Lu, Y.; Oladokun, M.; Lin, Z. Reducing the Exposure Risk in Hospital Wards by Applying Stratum Ventilation System. *Build Environ.* **2020**, *183*, 107204. [CrossRef]
20. Solidworks Flow Simulation Technical Reference Solidworks Flow Simulation. 2021. Available online: https://help.solidworks.com/2021/english/SolidWorks/cworks/r_solidworks_simulation_reference.htm (accessed on 5 June 2022).
21. Abhinav, R.; Sunder, P.B.S.; Gowrishankar, A.; Vignesh, S.; Vivek, M.; Kishore, V.R. Numerical Study on Effect of Vent Locations on Natural Convection in an Enclosure with an Internal Heat Source. *Int. Commun. Heat Mass Transf.* **2013**, *49*, 69–77. [CrossRef]
22. *Ashrae Standard 62.1-2010*; Ventilation for Acceptable Indoor Air Quality. ASHRAE Standard: Atlanta, GA, USA, 2010. Available online: https://www.lorisweb.com/LEEDv4/graphics/ASHRAE%20Standards/ASHRAE-D-86152%2062.1-2010.pdf (accessed on 12 September 2022).
23. Cho, J. Investigation on the Contaminant Distribution with Improved Ventilation System in Hospital Isolation Rooms: Effect of Supply and Exhaust Air Diffuser Configurations. *Appl. Therm. Eng.* **2019**, *148*, 208–218. [CrossRef] [PubMed]
24. Thatiparti, D.S.; Ghia, U.; Mead, K.R. Computational Fluid Dynamics Study on the Influence of an Alternate Ventilation Configuration on the Possible Flow Path of Infectious Cough Aerosols in a Mock Airborne Infection Isolation Room. *Sci. Technol. Built Environ.* **2017**, *23*, 355–366. [CrossRef] [PubMed]
25. Çuhadaroğlu, B.; Yiğit, Ş.; Sungurlu, C. ID 8-A CFD Analysis of Air Distributing Performance of a New Type HVAC Diffuser. In Proceedings of the CLIMAMED 2015, Juan Les Pins, France, 10–11 September 2015.
26. Mousavi, E. *Airborne Infection in Healthcare Environments: Implications to Hospital Corridor Design*; University of Nebraska: Lincoln, NE, USA, 2015; Available online: https://www.proquest.com/openview/af23e91396187791f139331f92ec66af/1?pq-origsite=gscholar&cbl=18750 (accessed on 15 March 2020).
27. Khosravi, G. Prediction of Bioparticles Dispersion and Distribution in a Hospital Isolation Room. Master's Thesis, École de Technologie Supérieure, Montréal, QC, Canada, 2016.
28. Hjermann, T.; Georges, L.; Tjelflaat, P. CFD Simulation of Active Displacement Ventilation. Master's Thesis, NTNU, Trondheim, Norway, 2017.
29. Ventilation of Health Care Facilities 170-2017. 2020. Available online: https://fgiguidelines.org/wp-content/uploads/2020/04/170_2017_n_20200303.pdf (accessed on 1 August 2022).
30. Ahmed, T. Performance Investigation of Building Ventilation System by Calculating Comfort Criteria through HVAC Simulation. *IOSR J. Mech. Civ. Eng.* **2012**, *3*, 7–12. [CrossRef]
31. Yoon, S.H.; Ahn, H.S.; Choi, Y.H. Numerical study to evaluate the characteristics of HVAC-related parameters to reduce CO_2 concentrations in cars. *Int. J. Automot. Technol.* **2016**, *17*, 959–966. [CrossRef]
32. Cehlin, M.; Moshfegh, B. Numerical Modeling of a Complex Diffuser in a Room with Displacement Ventilation. *Build Environ.* **2010**, *45*, 2240–2252. [CrossRef]
33. Cao, G.; Ruponen, M.; Paavilainen, R.; Kurnitski, J. Modelling and Simulation of the Near-Wall Velocity of a Turbulent Ceiling Attached Plane Jet after Its Impingement with the Corner. *Build Environ.* **2011**, *46*, 489–500. [CrossRef]
34. Gao, N.; Niu, J. Transient CFD Simulation of the Respiration Process and Inter-Person Exposure Assessment. *Build Environ.* **2006**, *41*, 1214–1222. [CrossRef]
35. Berlanga, F.A.; Olmedo, I.; de Adana, M.R.; Villafruela, J.M.; José, J.F.S.; Castro, F. Experimental Assessment of Different Mixing Air Ventilation Systems on Ventilation Performance and Exposure to Exhaled Contaminants in Hospital Rooms. *Energy Build* **2018**, *177*, 207–219. [CrossRef]
36. Ganesh, G.A.; Sinha, S.L.; Verma, T.N.; Dewangan, S.K. Numerical Investigation to Study the Effect of Inlet Inclination on the Turbulence Intensity of the Naturally Ventilated Room Using CFD. *Int. J. Eng. Adv. Technol.* **2020**, *9*, 583–589. Available online: https://www.researchgate.net/publication/357905704_Numerical_Investigation_to_Study_the_Effect_of_Inlet_Inclination_on_the_Turbulence_Intensity_of_the_Naturally_Ventilated_Room_Using_CFD (accessed on 13 November 2022). [CrossRef]
37. Karimipanah, T.; Awbi, H.B.; Moshfegh, B. Evaluating the Performance of Air Distribution Systems in Enclosures. In Proceedings of the 10th International Conference on Industrial Ventilation, Paris, France, 17–19 September 2012; p. 26.
38. Fabbri, K.; Gaspari, J.; Vandi, L. Indoor Thermal Comfort of Pregnant Women in Hospital: A Case Study Evidence. *Sustainability* **2019**, *11*, 6664. [CrossRef]
39. Rusly, E.; Airah, M.; Gagliardini, S.; Australia, T. *The Truth about the Air Diffusion Performance Index (ADPI)*; TROX Australia: North Sydney, Australia, 2014.